

# Facile approach to the fabrication of 3D electroconductive nanofibers with controlled size and conductivity templated by bacterial cellulose

Chuntao Chen · Yalin Yu · Kangming Li · Mengyao Zhao ·  
Lin Liu · Jiazhi Yang · Jian Liu · Dongping Sun

Received: 16 August 2015 / Accepted: 22 September 2015 / Published online: 28 September 2015  
© Springer Science+Business Media Dordrecht 2015

**Abstract** Controlled fabrication of biocompatible nanofibers with the required nanoscale and electrical performance can meet the needs of practical applications in biomedicine and electrochemistry. Here we report a high-performance 3D electroconductive nanomaterial templated by biocompatible bacterial cellulose (BC) nanofibers. Our approach can coat BC nanofibers with poly(3,4-ethylenedioxythiophene) (PEDOT) by in situ interfacial polymerization in a controllable manner, with average nanofiber diameters of 30–200 nm. PSS (poly(styrene sulfonate)) was doped to improve its conductivity in a controlled way. Mechanical performance and electrochemical measurements showed that the composite possesses excellent electroactive and mechanical stability. Especially evidence was provided that the BC/PEDOT

nanofibers with moderate PSS doping had excellent biocompatibility according to the results concerning the cellular morphology and proliferation of human mesenchymal stem cells cultured on the BC/PEDOT/PSS nanofibers. As a 3D conductive nanomaterial with flexibility, it shows potential application in electroactive substrates/scaffolds for tissue engineering, cell culture, biosensors, drug delivery and implanted electrodes.

**Keywords** Controllable fabrication · 3D nanofibers · Bacterial cellulose · Biocompatible · Electroconductive · Templated

## Introduction

In recent years, increasing attention has been focused on the fabrication of 3D (three-dimensional) conductive nanofibers for their unique properties and promising potential applications in biomedicine (Wei et al. 2005; Beneventi et al. 2006; Richardson-Burns et al. 2007; Li et al. 2009; Laforgue and Robitaille 2010). Due to the large length-diameter ratio, high specific area and prominent conductivity, electroactive and flexible nanofibers show potential application in tissue engineering, cell culture, biosensors, drug delivery and implanted electrodes (Xiao et al. 2004; Kim et al. 2006; Babakhani and Ivey 2010; Bai et al. 2011; Li et al. 2011; Ji et al. 2012; Jin et al. 2013).

---

C. Chen · L. Liu · J. Yang · D. Sun (✉)  
Institute of Chemicobiology and Functional Materials,  
Nanjing University of Science and Technology, 200 Xiao  
Ling Wei Street, Nanjing, Jiangsu Province, China  
e-mail: sundpe301@163.com

C. Chen · Y. Yu · K. Li · M. Zhao · L. Liu ·  
J. Yang · D. Sun  
School of Chemical Engineering, Nanjing University of  
Science and Technology, 200 Xiao Ling Wei Street,  
Nanjing, Jiangsu Province, China

J. Liu  
Institute of Functional Nano and Soft Materials  
(FUNSOM), Soochow University, 199 Ren Ai Road,  
Suzhou Industrial Park, Suzhou, Jiangsu Province, China

Compared with zero-, one- or two-dimensional nanomaterials, 3D electroactive nanomaterials have unique potential applications in biomedicine (Bai et al. 2011). Conductive nanofibers with diameters ranging from dozens to several hundred nanometers are remarkable for their unique nanometer size effect. However, there are only a few reports on 3D electroactive nanofibers with controlled electroactive and nanoscale size. Most previous reports on nanofiber fabrication are based on electrospinning and electrochemical deposition techniques (Wei et al. 2005; Kim et al. 2006; Li et al. 2006; Laforgue and Robitaille 2010; Xie et al. 2010; Müller et al. 2012; Jin et al. 2013; Shah et al. 2014; Wang et al. 2014). However, some inevitable limitations of these methods have appeared for biomedical applications, such as: (1) the size of these fibers is hard to control below 100 nm, being always several hundred nanometers to several micrometers; (2) producing nanofibers at small length scales with poor electroactive properties and biocompatibility; (3) uneven and nonuniform conduction of polymer distribution during the polymerization process. The synthesis of 3D nanomaterials in a controlled way is a fascinating topic in modern material science (Jin et al. 2014).

Traditional methods of fabricating 3D conductive nanofibers including blending, doping and coating with conductive materials such as conductive polymers, carbon nanotubes, graphene, inorganic nanoparticles and ionic liquids show a wide range of applications in many fields (Wei et al. 2005; Beneventi et al. 2006; Murugan et al. 2006; Li et al. 2009; Laforgue and Robitaille 2010; Bai et al. 2011; Müller et al. 2012; Farjana et al. 2013; Kim et al. 2013; De Salvi et al. 2014; Wu et al. 2014; Zhang et al. 2014). Compared with doping and blending, the conductive nanofibers fabricated by coating with conductive materials show the advantages of a high degree of porosity, high surface-to-volume ratio and relatively close structure mimicking the native extracellular matrix (ECM) (Xie et al. 2010; Shah et al. 2014; Wang et al. 2014). Poly(3,4-ethylenedioxythiophene) (PEDOT) is one of the most employed conductive polymers (Gupta et al. 2013; Zhang et al. 2013) because of its high conductivity and electrical stability (Wang et al. 2000). Bacterial cellulose (BC) is produced by many microorganisms and not only shows the properties of plant cellulose, but also has special properties such as high chemical purity and crystallinity, a high degree of polymerization ( $DP = 2000\text{--}8000$ ),

and excellent biocompatibility and biodegradability (Klemm et al. 2005; Huang et al. 2013). By coating conductive PEDOT onto hydrophilic biocompatible BC nanofibers, BC-templated 3D electroconductive composites can be easily obtained. Due to their attractive physical properties and continuous electrical performance, BC-templated conductive nanofibers promise a wide variety of applications (Klemm et al. 2011).

In this research, we describe a rapid, room temperature, in situ interfacial polymerization method to synthesize bulk quantities of a controlled electrically conducting 3D BC/PEDOT/PSS composite templated by BC nanofibers. The as-prepared 3D nanofibers showed homogeneous diameters in the range of 30–200 nm, which express an effective functional combination of the physicochemical properties and biocompatibility of BC and PEDOT/PSS. Various characterizations including FT-IR, TG and XPS were used to characterize the chemical structure. SEM was used to observe the 3D morphology. As the structure size and conductivity can be easily controlled by the polymerization time and temperature, there are clearly many more fields where this material can be applied. Evidence showed that the BC/PEDOT/PSS nanofibers had excellent biocompatibility from the results of the cellular morphology and proliferation of human mesenchymal stem cells (hMSCs) cultured on the BC/PEDOT/PSS nanofibers. They can provide 3D microenvironments between materials and cells well, as such composites can form a biocompatible interface and provide a biocompatible matrix or scaffold for a tissue-engineering scaffold. As nanofiber scaffolds exhibit many critical properties for tissue engineering, this template method provides a simple preparation process suitable for practical use.

## Experimental section

### Materials

BC hydrogel was cultivated using *Acetobacter xylinum* NUST4.2 (kept in our laboratory) through a static fermentation process (Sun et al. 2007) at 30 °C and then treated with 0.1 M NaOH solution at 80 °C for 2 h, followed by washing several times with distilled water until the pH became neutral. Ethanol, ether and sodium hydroxide were purchased from Sinopharm Chemical Reagent Co., Ltd., and were of

analytic grade. EDOT (99 %) and iron(III) chloride (99 %) were obtained from Sigma-Aldrich. All chemicals were used as received without further purification.

#### Preparation of BC/PEDOT/PSS composite materials

After cutting into the desired bulk, the sponge-like porous-structure BCs were immersed in a concentration series (0, 0.001, 0.01, 0.03, 0.05, 0.1, 0.5 and 1.0 M) of PSS water solution for 2 h. Then, the sponge-like porous-structure BC membrane was prepared using a simple freeze-drying method at  $-54\text{ }^{\circ}\text{C}$  for 24 h. The resultant BC aerogel was immersed in a series of EDOT ether solutions of gradient concentrations (0, 0.001, 0.0025, 0.005, 0.01, 0.025, 0.05  $\text{g ml}^{-1}$ ) at  $20\text{ }^{\circ}\text{C}$ . An  $\text{FeCl}_3$  ether solution (final concentration:  $0.05\text{ g ml}^{-1}$ ) was mixed as an oxidant species to initiate in situ interfacial polymerization of EDOT at the surface of BC nanofibers. The effect of different reaction times (0, 2, 5, 10, 15, 20, 25, 30, 45 min) was examined in relation to the interfacial polymerization. Finally, the BC/PEDOT nanofibers were washed with ethanol under ultrasonic oscillation (240 W, 42,000 Hz) to remove the residual reagents completely. The product samples were freeze-dried in a vacuum chamber for 24 h and stored at  $4\text{ }^{\circ}\text{C}$  before any subsequent test.

#### Characterization

We recorded the infrared spectra of materials on a Nicolet iS10 FTIR (Thermo Fisher Scientific, USA), and the wavenumbers ranged from 500 to  $4000\text{ cm}^{-1}$  by accumulating 32 scans at a resolution of  $4\text{ cm}^{-1}$ . Thermogravimetric analysis (TGA) was carried out on a NETZSCH STA 409 PC/PG system, a 5-mg sample was used for analyses in aluminum pans, and a dynamic nitrogen atmosphere between 50 and  $700\text{ }^{\circ}\text{C}$  was used throughout with a scanning rate of  $10\text{ K min}^{-1}$ . The  $\text{N}_2$  gas adsorption and desorption isotherms were obtained with ASAP 2020 (Micromeritics, USA), and a standard BET method (Brunauer et al. 1938) was used to calculate the pore size distribution and specific surface area. Scanning electron microscopy (SEM) micrographs were obtained with a Zeiss electron microscope (Supra 55, Carl Zeiss) at an acceleration voltage of 10 kV, and

the samples were covered with gold before the SEM analysis. XPS was carried out on an upgraded RBD PHI-5000C ESCA system (Perkin-Elmer) with Mg K radiation ( $h = 1253.6\text{ eV}$ ) and a pressure of  $1 \times 10^{-10}$  Torr. The neutral carbon 1s (C 1s) peak at 284.7 eV was referenced to compensate for surface charging effects of all binding energies. The four-probe method (MCP-T610, Mitsubishi Chemical Analytech) was used to measure the electrical conductivity of the BC/PEDOT/PSS nanofibers. Cyclic voltammetry (CV) and electrochemical impedance spectroscopy (EIS) measurements were performed by an electrochemical workstation (CHI660e, CH Instruments, Inc.). The nanofibers were tested as the working electrode, a saturated Ag/AgCl calomel electrode (SCE) as the reference electrode and a platinum electrode as the counter electrode; 0.1 M phosphate buffer solution (PBS) (pH 7.4) was used as the electrolyte solution. CV was scanned in potentials from  $-0.6$  to  $0.9\text{ V}$  at a scan rate of  $100\text{--}500\text{ mV s}^{-1}$ ; 0.1 M phosphate buffer solution (PBS) (pH 7.4) was used as the electrolyte solution. Electrochemical impedance spectroscopy (EIS) was measured over a frequency range of 0.1 to 100,000 Hz. Tensile stress-strain tests were performed on a Microcomputer Control Electronic Universal Testing Machine made by REGER in China (RGWT-4000-20), and the strain rate was  $20\text{ mm min}^{-1}$ . Tensile test specimens were prepared by cutting the membranes to 10 mm wide, 65 mm long strips using a precise cutter according to ASTM D-882-97 as a standard test method.

#### Cell proliferation and cytotoxicity test

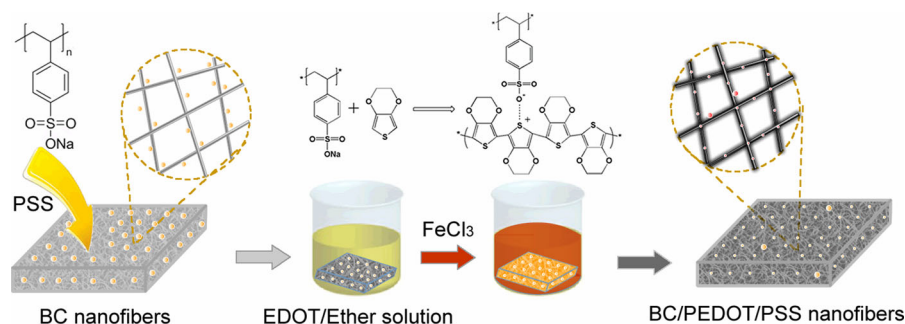
Human mesenchymal stem cells (hMSCs) were used as a model cell to evaluate the biocompatibility of the as-prepared nanofibers. All materials were cut into sections with 1.5 mm thickness, were immersed 30 min in 75 % ethanol-water (v/v) and underwent 30-min ultraviolet radiation before cell seeding. Several groups of materials (BC, BC/PEDOT and BC/PEDOT/PSS of different PSS concentrations) were placed in the center of the wells with the addition of 1 ml cell suspension to allow full attachment of cells to scaffolds, with each material setup investigated in three identical experiments. The hMSCs cells were cultured in DMEM, 10 % v/v FBS and 1 % v/v antibiotic/antimycotic solution and were incubated at  $37\text{ }^{\circ}\text{C}$  in 5 %  $\text{CO}_2$  for 7 days in 24-well TCPs at a cell

density of  $1.51 \times 10^4$  per well. Then the cell samples were sufficiently washed with PBS to remove excess nanoparticles. The cells were fixed with a 4 % formaldehyde solution and stained with a 4',6-diamidino-2-phenylindole (DAPI) solution. Immunocytochemistry of hMSCs was carried out using well-documented methods (Svensson et al. 2005; Dugan et al. 2010). The cell viabilities cultured on the nanofibers were examined using the standard methyl thiazolyl tetrazolium (MTT) assay (Hanelt et al. 1994). The fluorescent images were taken by a fluorescence microscope (Olympus) configured with Nuance CCD. The cells were fixed with 3 % glutaraldehyde for 2 h and dehydrated by incremental concentrations of ethanol solution (25, 50, 70, 80, 90, 95 % and absolute ethanol for 0.5 h each, v/v); subsequently, they were freeze-dried, and then the cell morphology was visualized by SEM.

## Results and discussion

### Fabrication of PSS-doped BC/PEDOT nanofibers

Conductive nanofibers are a binary composite material composed of BC and PEDOT, and sodium polystyrene sulfonate (PSS) is added as a dopant to improve the conductivity in a controlled way. Schematic 1 illustrates the fabrication procedure for the preparation of PSS-doped BC/PEDOT nanofibers. As shown in the schematic, BC gradually turns from white to black in ambient atmosphere. This color change indicates the progressive polymerization of EDOT on the BC nanofibers.



**Schematic 1** Schematic of BC/PEDOT 3D nanofiber fabrication. The polymerization of EDOT on the surface of BC nanofibers occurred as FeCl<sub>3</sub> helped EDOT oxidation in ether solution; a uniform PEDOT layer formed along the gradually declining interface between BC nanofibers. Before the

In Fig. 1a, the curve shows the relationship of the polymerization time and BC/PEDOT nanofiber average diameter and the relationship of the EDOT concentration and BC/PEDOT nanofiber average diameter. The systematically increasing concentration of PEDOT with increasing polymerization time suggested a significant thickness of PEDOT on BC nanofibers (as the AFM images in Fig. 2b show). With a certain concentration of  $0.01 \text{ g ml}^{-1}$  EDOT ether solution at  $20^\circ \text{C}$  polymerization for 10 min, a suitable condition to construct approximately 70-nm BC/PEDOT nanofibers was obtained, which contributed to an optimum specific surface area of  $266 \text{ m}^2 \text{ g}^{-1}$ , nearly three times that of pure BC nanofibers. The PEDOT shell layer did not break away from the BC nanofiber core by washing in water or ethanol even with ultrasonic (240 W, 42,000 Hz) processing, indicating an excellent binding force. This result indicates that this is an easy method to prepare conductive BC-templated 3D nanofibers with controlled size.

We then studied the relationship of the PSS doped concentration and the conductivity of the nanofibers, as Fig. 2 shows. The curve in Fig. 2a shows that a PSS doping concentration of 0.05 M can effectively increase the conductivity from  $0.001$  to  $0.1 \text{ S cm}^{-1}$  as a result of the positive PEDOT<sup>+</sup> sites in the doped polymer conjugated with negative PSS<sup>-</sup> counter ions. The charge distribution along a partly oxidized PEDOT-PSS chain results in a broad distribution of binding energies for the sulfur atoms, resulting in an asymmetric tail on the higher binding energy side of the (neutral) PEDOT sulfur signal (Greczynski et al. 1999). The stable form of PEDOT/PSS in BC provided an electrode layer with a more stable and higher

polymerization of EDOT on the BC nanofibers, the sponge-like porous-structure BC was immersed in a concentration series (0.01, 0.05, 0.1, 0.3, 0.5, 0.8 and 1.0 M) of PSS water solution to study the effect of the PSS concentration on the conductivity of BC/PEDOT

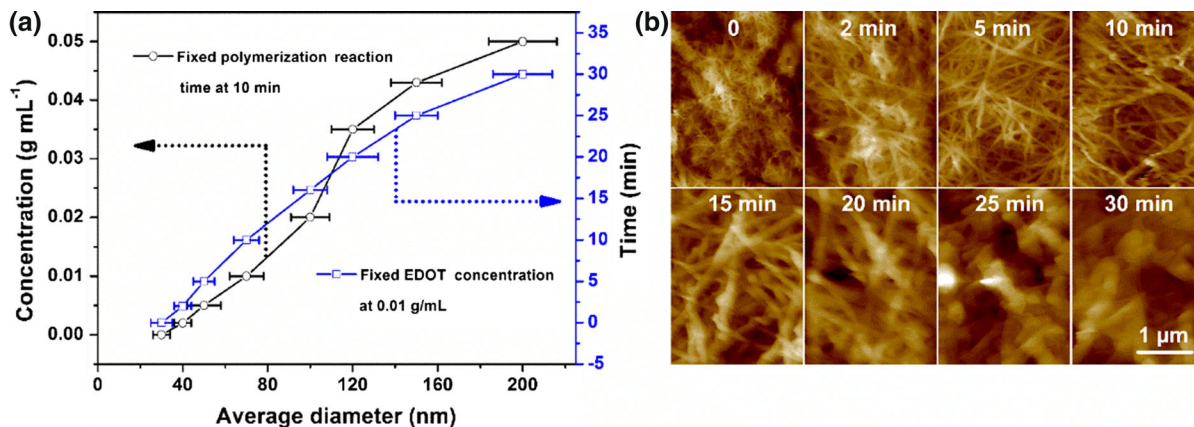


**Fig. 1** a The relationships between polymerization time (blue curve) and EDOT concentration (black curve) with BC/PEDOT nanofiber average diameter and the AFM images (b)

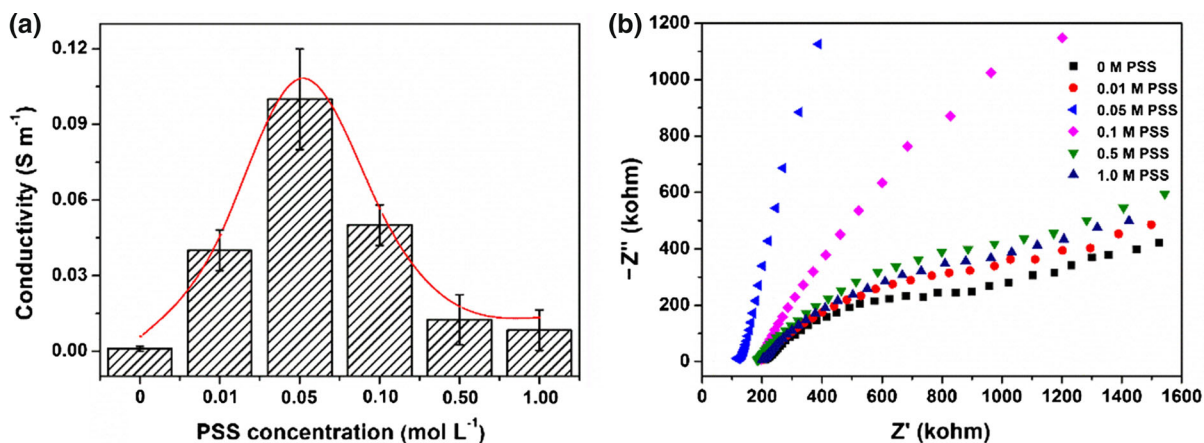


**Fig. 2** a The effect of PSS concentration on the conductivity of BC/PEDOT; b EIS curve of BC/PEDOT nanofibers with different concentrations of PSS doped, 1–100,000 Hz

conductivity for electrical signal transmission. We then used electrochemical impedance spectroscopy (EIS) to determine the charge-transfer resistance as indicated by the diameter of the preceding semicircle in the Nyquist plot (Fig. 2b) (Zhao et al. 2003). From Fig. 2b, we also see the impedance value changes with increasing PSS concentration, and with 0.05 M PSS doped we obtained the lowest resistance, suggesting the best electrical property. Figure 2a shows that with increasing PSS concentration the electrical conductivity increases, reaching the highest electrical conductivity of the nanocomposite with 0.05 M PSS. However, above this PSS concentration the electrical conductivity decreases. We think the decrease of the conductivity was caused by the extreme 3D structural

damage of excessive (above 0.5 M) doped PSS from the morphology of the BC, BC/PEDOT and BC/PEDOT/PSS composite material by SEM. Moreover, the excessive doped PSS may disturb the polymerization reaction of EDOT on the BC nanofiber, resulting in a thinner PEDOT coating layer, and decreasing the electrical conductivity. This result gives us an easy way to prepare conductive BC-templated materials with controlled electrical conductivity.

### Morphology

The morphology of BC and BC/PEDOT composite materials with and without PSS doping was imaged via SEM. A different synthesis procedure results in

quite different structures from those of BC and plant cellulose. Figure 3 presents typical SEM images of freeze-dried BC (Fig. 3a) and the BC/PEDOT composite with (Fig. 3b) and without PSS doping (Fig. 3c). A well-organized 3D network structure could be observed with BC. After immersion into the EDOT solution, BC fibrils became bigger as a result of the coverage of PEDOT on the fiber surface. Compared with BC nanofibers, which have an average diameter of about 30–50 nm, the core-shell structures of BC/PEDOT and BC/PEDOT/PSS show homogeneous diameters in the range of 40–200 nm. The yellow arrow in Fig. 3c shows the excess spherical PSS. Although the doped PSS can greatly increase the total electrical conductivity of BC/PEDOT nanofibers, excessive doped PSS may disturb the polymerization reaction of EDOT on BC nanofibers, resulting in thinner nanofibers, as Fig. 3c shows. Thus, we can draw the conclusion that the doped PSS in BC/PEDOT nanofibers not only affects its conductivity, but also impacts its morphology. Thus, the doping of PSS may be a good way to control fabricating the required size and conductivity of 3D nanofibers.

#### Chemical structure and elements

FT-IR was used to analyze the chemical structure of BC, BC/PEDOT and BC/PEDOT/PSS nanofibers. The

bands at 3345, 2890, 1648, 1429 and 1033  $\text{cm}^{-1}$ , as Fig. 4a shows, are associated with native BC (D'Arcy et al. 2014). The peak assignment of the BC/PEDOT/PSS complex were: stretching vibration peaks of C–C and C=C at of 1314 and 1523  $\text{cm}^{-1}$ , respectively; C–S peaks at 987, 926 and 845  $\text{cm}^{-1}$ ; C–O–C peaks at 1202, 1150 and 1057  $\text{cm}^{-1}$ ; the vibration peak of C–O–CH<sub>2</sub>–CH<sub>2</sub>–O–C at 1150  $\text{cm}^{-1}$  (Kvarnström et al. 1999). The three peak absorptions at 1642, 1433 and 1433  $\text{cm}^{-1}$  can be assigned to the thiophene ring, which confirms the existence of PEDOT. The peak at 1202–1170  $\text{cm}^{-1}$  is a characteristic absorption of SO<sup>3-</sup> confirming the existence of PSS. We then analyzed the thermal stability and thermal decomposition of BC, BC/PEDOT and BC/PEDOT/PSS. As seen in Fig. 4b, the first slight weight loss of the pure BC, BC/PEDOT and BC/PEDOT/PSS occurring at 50–100 °C is due to water loss. The second weight loss of BC occurring at 340–380 °C is a result of BC splitting. In the case of BC/PEDOT and BC/PEDOT/PSS, the second weight loss occurred rapidly at 280–320 °C and 320–360 °C, respectively, earlier than that of BC. More residues were recorded at up to 700 °C for BC/PEDOT and BC/PEDOT/PSS compared with BC, demonstrating the existence of PEDOT and PEDOT/PSS. The thermal degradation temperature may be affected by the structural parameters such as molecular weight, crystallinity and orientation.

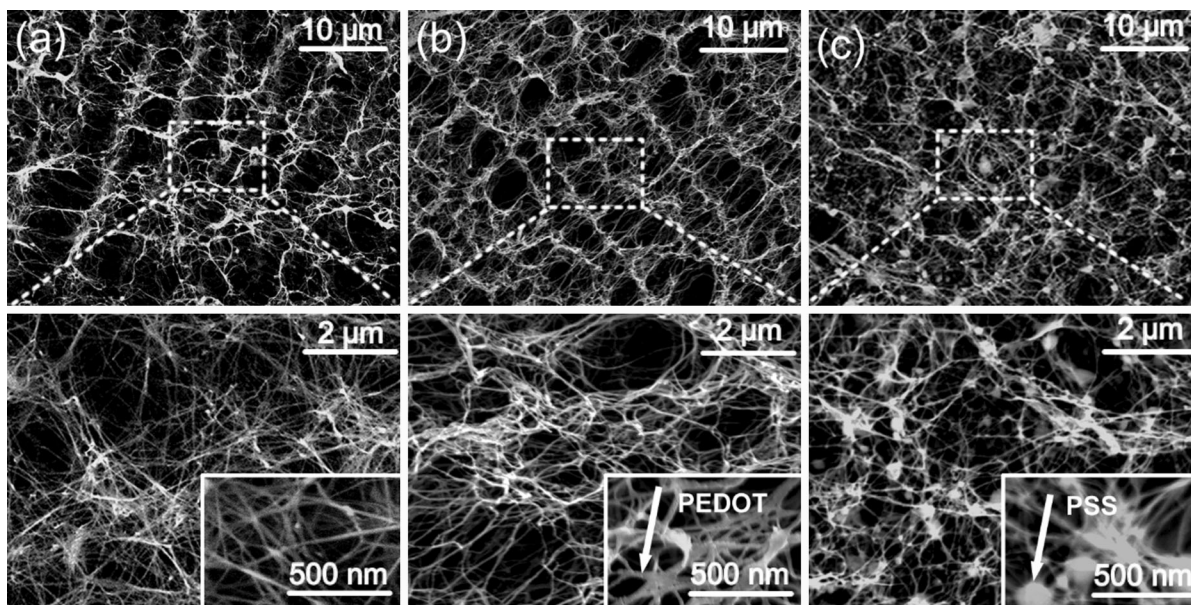


**Fig. 3** SEM images of 3D BC (a), 3D BC/PEDOT (b) and 3D BC/PEDOT/PSS (c) nanofibers of different magnifications

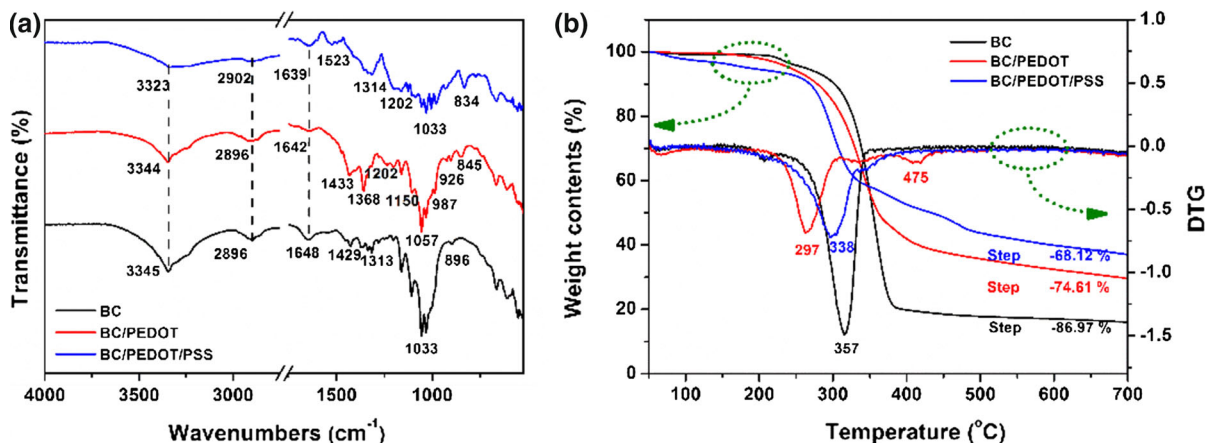


**Fig. 4** FT-IR (a) and TG (b) curves of BC BC/PEDOT and BC/PEDOT/PSS

We then obtained the element distribution of BC/PEDOT/PSS from X-ray photoelectron spectroscopy (Fig. 5a). The characteristic peaks of PEDOT are C–S (285.3 eV) in the  $\alpha$  position, C–O–C (286.3 eV) in the  $\beta$  position and C–O–C (286.9 eV) bonding in the ethylene bridge (Fig. 5b), in perfect accordance with the values reported by Jönsson et al. (2003). With 1.2 eV energy splitting and a 1:2 intensity ratio, peaks S 2p<sub>3/2</sub> and S 2p<sub>1/2</sub> (Fig. 5c) both involve contributions from a spin split doublet (Castner et al. 1996). The contribution peaks S 2p correspond to sulfur atoms of the PEDOT at 163.0 and 164.2 eV. Peaks at 167.7 and 168.9 eV at higher binding energies belong to PSS because of the electronegative oxygen atom attached to the electropositivity sulfur atom in the PSS sulfonate fragment (Schaarschmidt et al. 2009). Apart from oxidation, some Fe<sup>2+</sup> from FeCl<sub>3</sub> (Fig. 5d) may act as doped ions during the polymerization of EDOT. The Fe 2p<sub>3</sub> and 2p<sub>1</sub> contribution peaks at 711.7 and 724.9 eV may result in better electrical conductivity.

#### Electrochemical and mechanical characteristics

The optimal mechanical properties of the BC, BC/PEDOT and BC/PEDOT/PSS nanofibers were obtained as shown in Fig. 6a. The tensile strength and Young's modulus of BC nanofibers were  $3.30 \pm 0.6$  and  $1.29 \pm 0.4$  MPa, respectively, while BC/PEDOT nanofibers were  $4.00 \pm 0.6$  and  $0.83 \pm 0.2$  MPa and BC/PEDOT/PSS were  $4.36 \pm 0.8$  and  $0.99 \pm 0.2$  MPa, respectively, as Table 1 shows. The incorporation of PEDOT/PSS could affect the orientation of BC nanofibers (Jönsson et al. 2003).

Consequently, this incomplete orientation decreases the crystallinity of BC, which in turn leads to a decrease in the modulus. At the same time, PEDOT can give more space for BC chains when applying stress, acting as a plasticizer, where the PSS can act as a cross-bonding molecule, resulting in decreased elongation (Jönsson et al. 2003). To test the electrochemical performance of 3D BC, BC/PEDOT and BC/PEDOT/PSS nanofibers, their CVs measured in PBS solution (0.1 M, pH 7.4) using a three-electrode system is shown in Fig. 6b. As an insulator with a conductivity of  $10^{-8}$  S cm<sup>-1</sup>, the CV of pure BC is linear (Fig. 6b) (Müller et al. 2012). The potential of the BC/PEDOT/PSS electrode bias cycling from negative to positive and back reflects the intrinsic redox reaction of the nanofiber material. This propels ion exchange between the electrode and the electrolyte moving mobile charge carriers in and out of the PEDOT/PSS matrix. The stable form of PEDOT/PSS in BC provided an electrode layer with a more stable and higher conductivity for electrical signal transmission. The CV comparison of the three samples indicated that the incorporation of the conducting polymer could enhance the electrical properties. These results demonstrate that the fabricated devices possess excellent flexibility and mechanical stability.

#### Biocompatibility

In order to evaluate the possibility of applying these nanofibers in biotechnology, human mesenchymal stem cells (hMSCs) were used to examine the biocompatibility of the nanofibers. Figure 7a shows

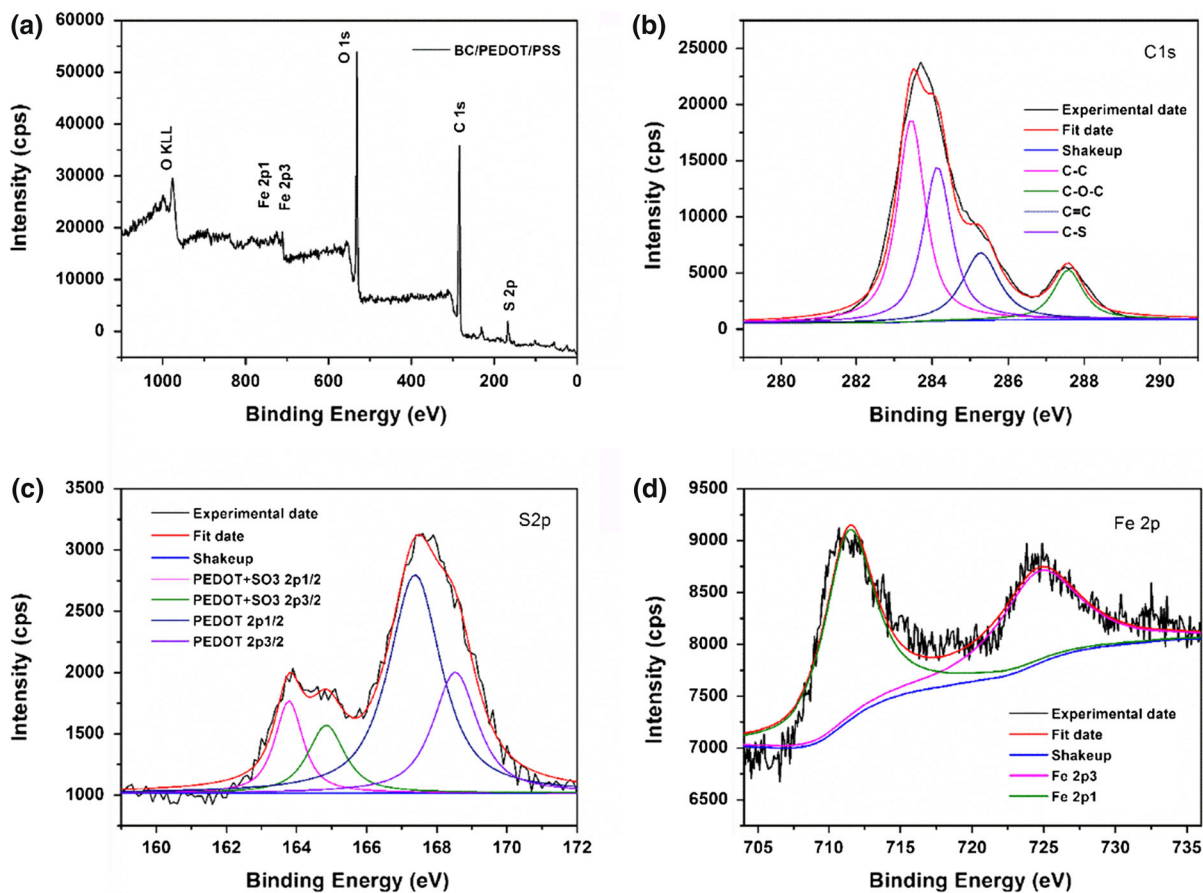


Fig. 5 XPS a of BC/PEDOT/PSS and their b C1s, c S2p and d Fe2p resolution results

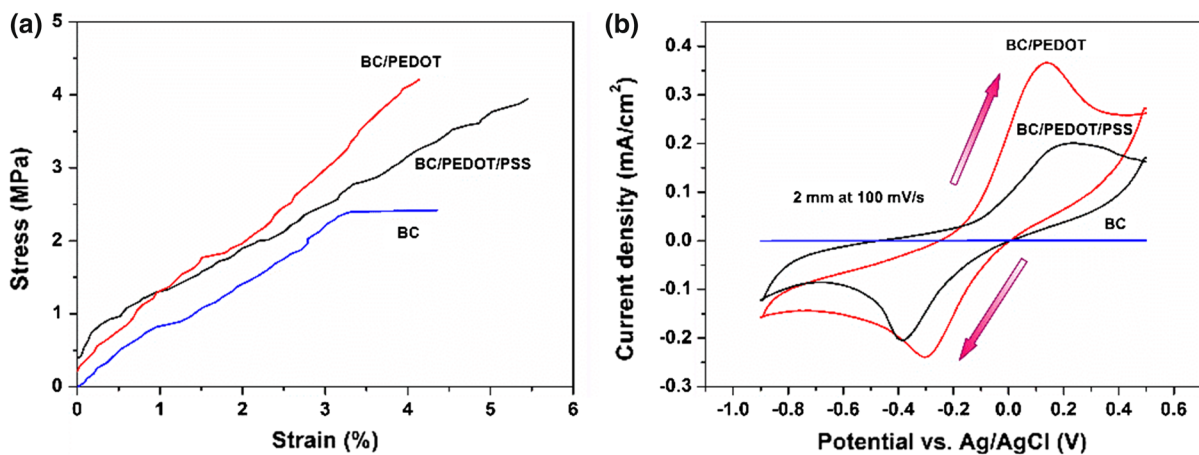


Fig. 6 a Stress-strain curves for tensile tests on BC and BC/PEDOT nanofibers; b CVs recorded at the BC, BC/PEDOT and BC/PEDOT/PSS nanofibers in the 0.1 M PBS buffer solution



**Table 1** Stress-strain data of the tensile test result on BC and BC/PEDOT with and without PSS doping

Sample name	Young's modulus (MPa)	Tensile strength (MPa)	Elongation at break (%)
BC	1.29 ± 0.4	3.30 ± 0.6	2.56 ± 0.5
BC/PEDOT	0.83 ± 0.2	4.00 ± 0.6	4.82 ± 0.6
BC/PEDOT/PSS	0.99 ± 0.2	4.36 ± 0.8	4.32 ± 0.6

the colored hMSCs by DAPI and FITC after culture on BC nanofibers and BC/PEDOT nanofibers with and without PSS doping after 7 days. The approximate number of hMSCs on BC/PEDOT/PSS-0.01 M and BC/PEDOT as BC revealed an excellent

biocompatibility. Many well-developed, brightly stained focal adhesions were observed on all of the BC/PEDOT and BC/PEDOT/PSS-0.01 M nanofiber surface types. With an increasing PSS doping concentration, an added toxicity to cells could be

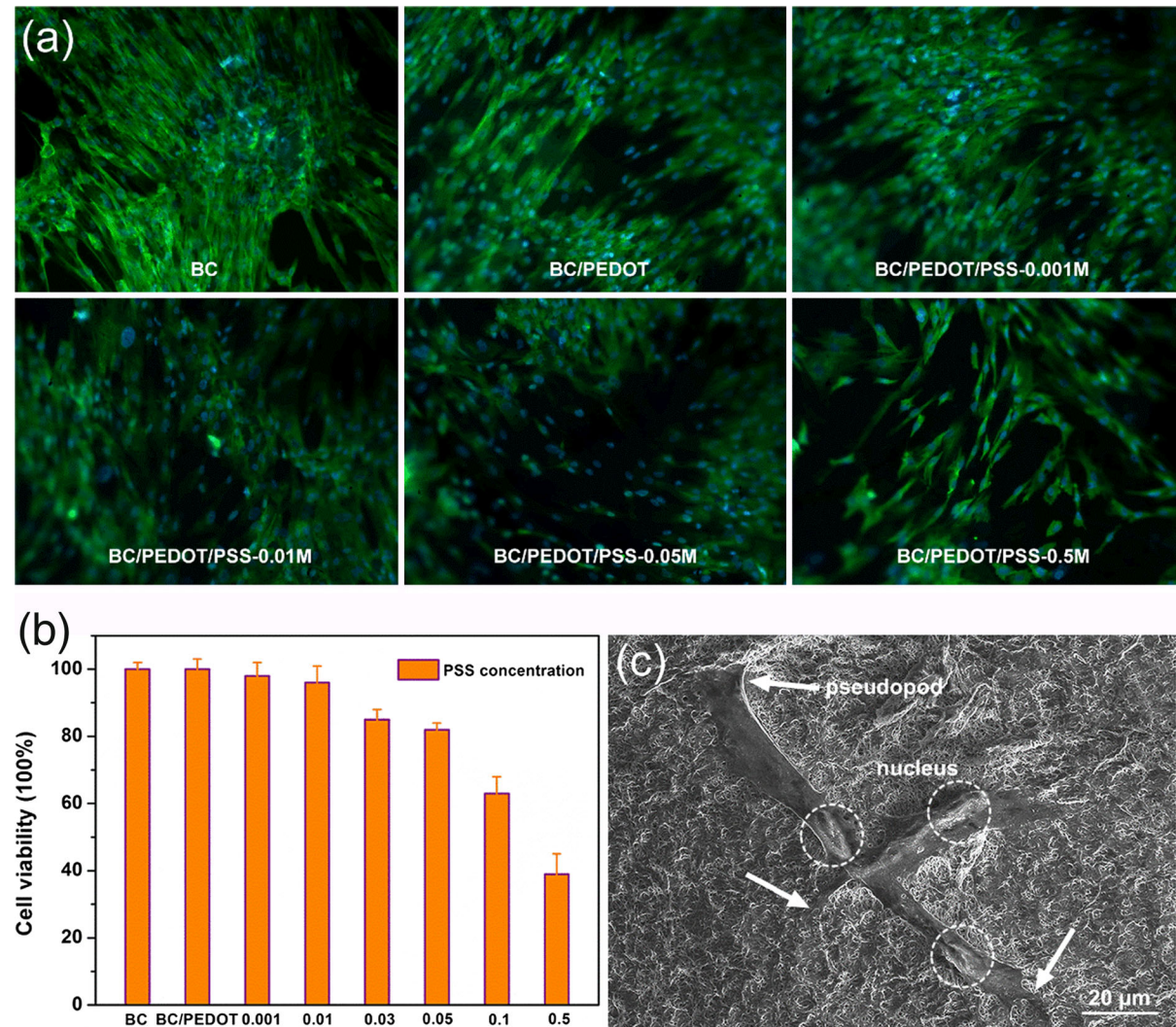


**Fig. 7** Fluorescence and SEM images of hMSCs cultured on different scaffolds at day 7. **a** Fluorescence images of hMSCs cultured on a glass sheet, BC nanofibers, BC/PEDOT nanofibers and BC/PEDOT/PSS at day 7; **b** cell viability of hMSCs on a

glass sheet, BC, BC/PEDOT and BC/PEDOT/PSS nanofibers; hMSCs were originally seeded at  $1.51 \times 10^4$  cells/cm<sup>2</sup>; **c** SEM image of hMSCs on BC/PEDOT/PSS nanofibers (mean ± SD,  $n = 3$ )

observed. However, still 80 % cells could be alive when the PSS concentration increased to 0.05 M. Therefore, a PSS-doped concentration below 0.05 M can be regarded as having low cell cytotoxicity.

hMSCs were stained on the scaffolds after 7 days of culture to examine the cell activity on different scaffolds. Cell attachment and proliferation on these scaffolds were analyzed with the standard methyl thiazolyl tetrazolium (MTT) assay. As shown in Fig. 7b, after 7 days, the cell viability of BC/PEDOT and BC/PEDOT/PSS-0.01 M was the same as on BC. These results strongly supported that the roughness of the PEDOT structure with deep interconnected pores could promote cell proliferation. Furthermore, from the quantitative viability test results of cells adhered on these different substrates, the BC/PEDOT and BC/PEDOT/PSS nanofiber substrate developed significant hMSC attachment, the same as the pure BC substrate.

From Fig. 7c we can see the hMSC growth form on the BC/PEDOT/PSS surface. They formed a layer on the surface, and many pseudopodia grew along the nanofibers. Therefore, the cells stretched their morphology on the nanofibers and proliferated. This preliminary experiment suggests that the BC/PEDOT composite with 0.01 M PSS doping has a similar biocompatibility to pure BC and BC/PEDOT in terms of cell culture, resulting in better 3D microenvironments as such composites can form a biocompatible interface between nanofibers and cells.

## Conclusions

In this research, a biocompatible 3D nanofiber with excellent mechanical and electrical performance templated by bacterial cellulose was prepared in a controlled manner. SEM images showed it kept a well-organized 3D network structure. From the electrochemical and mechanical property tests, the BC/PEDOT/PSS nanofibers showed excellent and stable performance. Such flexible and mechanically robust BC/PEDOT/PSS nanofibers displaying a controlled size and stable electroactive behavior could find a wide range of applications in electrically stimulated drug release devices, implantable biosensors and neuronal prostheses. Considering the excellent biocompatibility of BC/PEDOT/PSS, with future

work, we believe that this 3D nanofiber will find applications in regenerative medicine and in improving the understanding of tissue development.

**Acknowledgments** This work was supported by the Advanced Catalysis and Green Manufacturing Collaborative Innovation Centre, Synergetic Research Centre for Advanced Micro-Nano Materials and Technology of Jiangsu Province and the Qing Lan Project. It was funded by the National Natural Science Foundation of China (grants 51272106), the Fundamental Research Funds for the Central Universities (grant 30920130121001), Research Fund for the Doctoral Program of Higher Education of China (RFDP) (grant 20123219110015) and the Priority Academic Program Development of Jiangsu Higher Education Institutions (PAPD, China).

## References

- Babakhani B, Ivey DG (2010) Improved capacitive behavior of electrochemically synthesized Mn oxide/PEDOT electrodes utilized as electrochemical capacitors. *Electrochim Acta* 55(12):4014–4024
- Bai X, Hu X, Zhou S, Yan J, Sun C, Chen P, Li L (2011) Controlled fabrication of highly conductive three-dimensional flowerlike poly(3,4-ethylenedioxythiophene) nanostructures. *J Mater Chem A* 21(20):7123–7129
- Beneventi D, Alila S, Boufi S, Chaussy D, Nortier P (2006) Polymerization of pyrrole on cellulose fibres using a FeCl<sub>3</sub> impregnation- pyrrole polymerization sequence. *Cellulose* 13(6):725–734
- Brunauer S, Emmett PH, Teller E (1938) Adsorption of gases in multimolecular layers. *J Am Chem Soc* 60(2):309–319
- Castner DG, Hinds K, Grainger DW (1996) X-ray photoelectron spectroscopy sulfur 2p study of organic thiol and disulfide binding interactions with gold surfaces. *Langmuir* 12(21):5083–5086
- D'Arcy JM, El-Kady MF, Khine PP, Zhang L, Lee SH, Davis NR, Liu DS, Yeung MT, Kim SY, Turner CL (2014) Vapor-phase polymerization of nanofibrillar poly(3,4-ethylenedioxythiophene) for supercapacitors. *ACS Nano* 8(2):1500–1510
- De Salvi DTB, Barud HS, Pawlicka A, Mattos RI, Raphael E, Messaddeq Y, Ribeiro SJL (2014) Bacterial cellulose/triethanolamine based ion-conducting membranes. *Cellulose* 21(3):1975–1985
- Dugan JM, Gough JE, Eichhorn SJ (2010) Directing the morphology and differentiation of skeletal muscle cells using oriented cellulose nanowhiskers. *Biomacromolecules* 11(9):2498–2504
- Farjana S, Toomadj F, Lundgren P, Sanz-Velasco A, Naboka O, Enoksson P (2013) Conductivity-dependent strain response of carbon nanotube treated bacterial nanocellulose. *J Sens* 2013:1–7
- Greczynski G, Kugler T, Salaneck W (1999) Characterization of the PEDOT-PSS system by means of X-ray and ultraviolet photoelectron spectroscopy. *Thin Solid Films* 354(1):129–135

- Gupta D, Wienk MM, Janssen RA (2013) Efficient polymer solar cells on opaque substrates with a laminated PEDOT: PSS top electrode. *Adv Energy Mater* 3(6):782–787
- Hanelt M, Gareis M, Kollarczik B (1994) Cytotoxicity of mycotoxins evaluated by the MTT-cell culture assay. *Mycopathologia* 128(3):167–174
- Huang Y, Zhu C, Yang J, Nie Y, Chen C, Sun D (2013) Recent advances in bacterial cellulose. *Cellulose* 21(1):1–30
- Ji H, Zhang L, Pettes MT, Li H, Chen S, Shi L, Piner R, Ruoff RS (2012) Ultrathin graphite foam: a three-dimensional conductive network for battery electrodes. *Nano Lett* 12(5):2446–2451
- Jin L, Wang T, Feng Z-Q, Leach MK, Wu J, Mo S, Jiang Q (2013) A facile approach for the fabrication of core-shell PEDOT nanofiber mats with superior mechanical properties and biocompatibility. *J Mater Chem B* 1(13):1818–1825
- Jin L, Feng Z-Q, Wang T, Ren Z, Ma S, Wu J, Sun D (2014) A novel fluffy hydroxylapatite fiber scaffold with deep interconnected pores designed for three-dimensional cell culture. *J Mater Chem B* 2(1):129–136
- Jönsson S, de Jong MP, Groenendaal L, Salaneck WR, Fahlman M (2003) Phenyl-capped EDOT trimer: its chemical and electronic structure and its interface with aluminum. *J Phys Chem B* 107(39):10793–10800
- Kim C, Yang KS, Kojima M, Yoshida K, Kim YJ, Kim YA, Endo M (2006) Fabrication of electrospinning-derived carbon nanofiber webs for the anode material of lithium-ion secondary batteries. *Adv Funct Mater* 16(18):2393–2397
- Kim S-S, Jeon J-H, Kee C-D, Oh I-K (2013) Electro-active hybrid actuators based on freeze-dried bacterial cellulose and PEDOT:PSS. *Smart Mater Struct* 22(8):085026
- Klemm D, Heublein B, Fink H-P, Bohn A (2005) Cellulose: fascinating biopolymer and sustainable raw material. *Angew Chem Int Ed Engl* 44(22):3358–3393
- Klemm D, Kramer F, Moritz S, Lindstrom T, Ankerfors M, Gray D, Dorris A (2011) Nanocelluloses: a new family of nature-based materials. *Angew Chem Int Ed Engl* 50(24):5438–5466
- Kvarnström C, Neugebauer H, Blomquist S, Ahonen H, Kankare J, Ivaska A (1999) In situ spectroelectrochemical characterization of poly(3,4-ethylenedioxythiophene). *Electrochim Acta* 44(16):2739–2750
- Laforge A, Robitaille L (2010) Production of conductive PEDOT nanofibers by the combination of electrospinning and vapor-phase polymerization. *Macromolecules* 43(9):4194–4200
- Li M, Guo Y, Wei Y, MacDiarmid AG, Lelkes PI (2006) Electrospinning polyaniline-contained gelatin nanofibers for tissue engineering applications. *Biomaterials* 27(13):2705–2715
- Li L, Huang Y, Yan G, Liu F, Huang Z, Ma Z (2009) Poly(3,4-ethylenedioxythiophene) nanospheres synthesized in magnetic ionic liquid. *Mater Lett* 63(1):8–10
- Li J, Vadahanambi S, Kee CD, Oh IK (2011) Electrospun fullerenol-cellulose biocompatible actuators. *Biomacromolecules* 12(6):2048–2054
- Müller D, Mandelli JS, Marins JA, Soares BG, Porto LM, Rambo CR, Barra GMO (2012) Electrically conducting nanocomposites: preparation and properties of polyaniline (PANI)-coated bacterial cellulose nanofibers (BC). *Cellulose* 19(5):1645–1654
- Murugan AV, Quintin M, Delville M-H, Campet G, Gopinath CS, Vijayamohan K (2006) Exfoliation-induced nanoribbon formation of poly(3,4-ethylene dioxothiophene) PEDOT between MoS<sub>2</sub> layers as cathode material for lithium batteries. *J Power Sources* 156(2):615–619
- Richardson-Burns SM, Hendricks JL, Foster B, Povlich LK, Kim DH, Martin DC (2007) Polymerization of the conducting polymer poly(3,4-ethylenedioxythiophene) (PEDOT) around living neural cells. *Biomaterials* 28(8):1539–1552
- Schaarschmidt A, Farah AA, Aby A, Helmy AS (2009) Influence of nonadiabatic annealing on the morphology and molecular structure of PEDOT-PSS films. *J Phys Chem B* 113(28):9352–9355
- Shah S, Yin PT, Uehara TM, Chueng ST, Yang L, Lee KB (2014) Guiding stem cell differentiation into oligodendrocytes using graphene-nanofiber hybrid scaffolds. *Adv Mater* 26(22):3673–3680
- Sun D, Zhou L, Wu Q, Yang S (2007) Preliminary research on structure and properties of nano-cellulose. *J Wuhan Univ Technol Mater Sci Ed* 22(4):677–680
- Svensson A, Nicklasson E, Harrah T, Panilaitis B, Kaplan D, Brittberg M, Gatenholm P (2005) Bacterial cellulose as a potential scaffold for tissue engineering of cartilage. *Biomaterials* 26(4):419–431
- Wang C, Kilitziraki M, MacBride JH, Bryce M, Horsburgh L, Sheridan A, Monkman A, Samuel I (2000) Tuning the optoelectronic properties of pyridine-containing polymers for light-emitting devices. *Adv Mater* 12(3):217–222
- Wang J, Wang L, Yang M, Zhu Y, Tomsia A, Mao C (2014) Untangling the effects of peptide sequences and nanotopographies in a biomimetic niche for directed differentiation of iPSCs by assemblies of genetically engineered viral nanofibers. *Nano Lett* 14(12):6850–6856
- Wei M, Lee J, Kang B, Mead J (2005) Preparation of core-sheath nanofibers from conducting polymer blends. *Macromol Rapid Commun* 26(14):1127–1132
- Wu F, Wang Y, Wang M (2014) Using organic solvent absorption as a self-assembly method to synthesize three-dimensional (3D) reduced graphene oxide (RGO)/poly(3,4-ethylenedioxythiophene) (PEDOT) architecture and its electromagnetic absorption properties. *RSC Adv* 4(91):49780–49782
- Xiao Y, Cui X, Martin DC (2004) Electrochemical polymerization and properties of PEDOT/S-EDOT on neural microelectrode arrays. *J Electroanal Chem* 573(1):43–48
- Xie J, MacEwan MR, Schwartz AG, Xia Y (2010) Electrospun nanofibers for neural tissue engineering. *Nanoscale* 2(1):35–44
- Zhang W, Zhao B, He Z, Zhao X, Wang H, Yang S, Wu H, Cao Y (2013) High-efficiency ITO-free polymer solar cells using highly conductive PEDOT:PSS/surfactant bilayer transparent anodes. *Energy Environ Sci* 6(6):1956–1964
- Zhang Q, Xu D, Zhou X, Wu X, Zhang K (2014) In situ synthesis of CuO and Cu nanostructures with promising electrochemical and wettability properties. *Small* 10(5):935–943
- Zhao G-C, Zhang L, Wei X-W, Yang Z-S (2003) Myoglobin on multi-walled carbon nanotubes modified electrode: direct electrochemistry and electrocatalysis. *Electrochem Commun* 5(9):825–829